Supplementary Information for

Discovery of Intrinsic Magnetospheric Ion Behavior at Mars

Chi Zhang[1,2], Hans Nilsson[3], Yusuke Ebihara[4], Masatoshi Yamauchi[3], Moa Persson[5], Zhaojin Rong[1,2,*], Jun Zhong[1,2], Chuanfei Dong[6], Yuxi Chen[6], Xuzhi Zhou[7], Yixin Sun[7], Yuki Harada[8], Jasper Halekas[9], Shaosui Xu[10], Yoshifumi Futaana[3], Zhen Shi[1,2], Chongjing Yuan[1,2], Xiaotong Yun[11], Song Fu[11], Jiawei Gao[1,2], Mats Holmström[3], Yong Wei[1,2,*], and Stas Barabash[3]

[1]Key Laboratory of Earth and Planetary Physics, Institute of Geology and Geophysics, Chinese Academy of Sciences, Beijing, China

[2]College of Earth and Planetary Sciences, University of Chinese Academy of Sciences, Beijing, China

[3]Swedish Institute of Space Physics, Kiruna, Sweden

[4]Research Institute for Sustainable Humanosphere, Kyoto University, Uji, Japan

[5]Graduate School of Frontier Sciences, The University of Tokyo, Kashiwa, Japan

[6]Department of Astronomy, Boston University, Boston, MA, USA

[7]School of Earth and Space Sciences, Peking University, Beijing, China

[8]Department of Geophysics, Graduate School of Science, Kyoto University, Kyoto, Japan

[9]Department of Physics and Astronomy, University of Iowa, Iowa City, IA, USA

[10]Space Sciences Laboratory, University of California, Berkeley, Berkeley, CA, USA

[11]Department of Space Physics, School of Electronic Information, Wuhan University, Wuhan, China

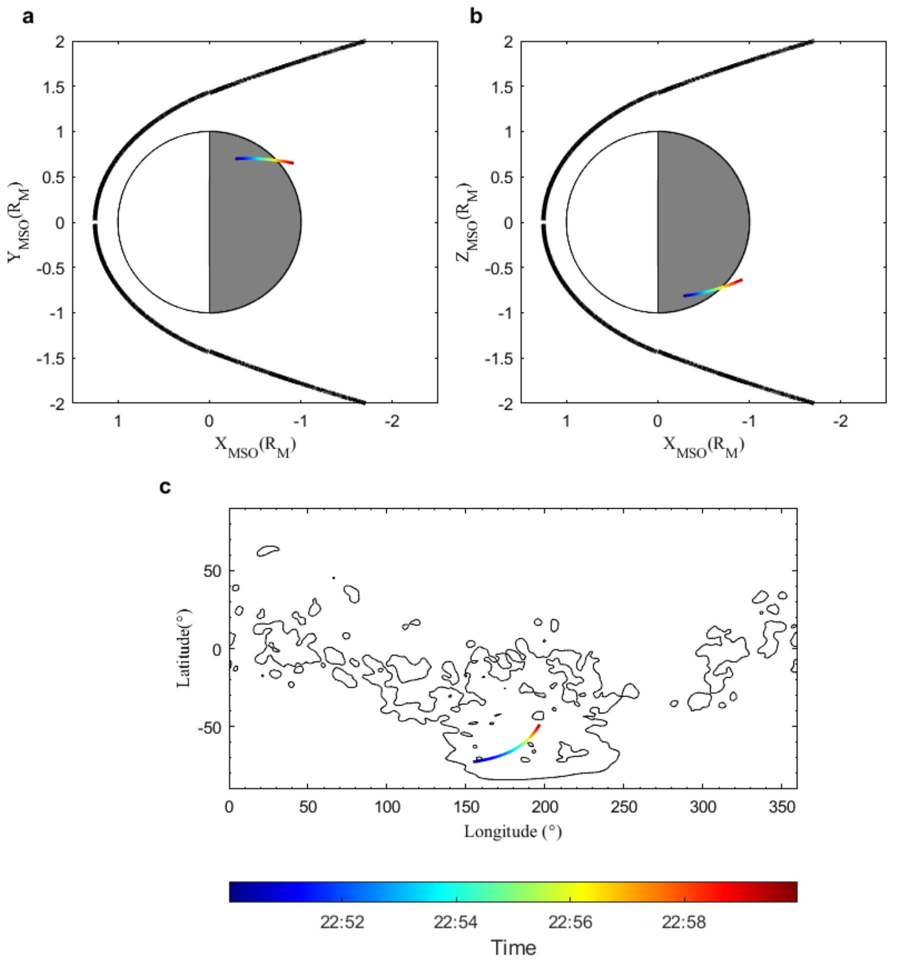

Supplementary Figure 1. (a), (b), and (c) show the trajectory of MAVEN in the $X_{MSO} - Y_{MSO}$, $X_{MSO} - Z_{MSO}$, and in Geographic coordinates, respectively, during 22:50-23:00 UTC on April 15, 2018. The black dashed curves in (a), (b) denote the nominal magnetic pile-up boundary from Trotignon et al. (2006). The black contour lines in (c) represents the crustal fields at an altitude of 180 km from the latest crustal fields model (Gao et al. 2021). The colored curves represent the time along the trajectory of MAVEN.

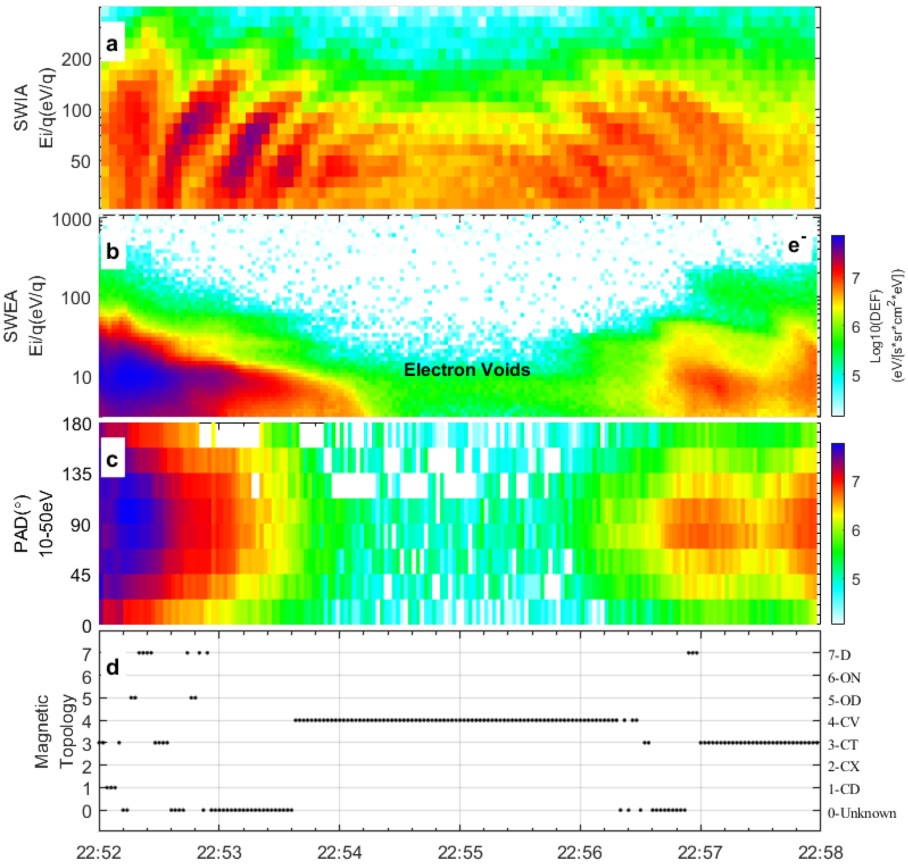

Supplementary Figure 2. Electron distributions and magnetic topology analysis. **a:** Ion spectrum. **b:** Electron spectrum observed by SWEA. **c:** The pitch angle distribution of 10-50 eV electrons. **d**: the magnetic topology index calculated via the method provided by Xu et al. (2019). It can be seen that the electrons show a double-sided loss cone distribution, implying that the field lines were closed and connected to the ionosphere. Apart from the unknown types, the magnetic field lines basically belong to the closed-voids (CV) and closed-trapped (C-T) types, which both are the closed crustal field lines with both foot-points located in the ionosphere.

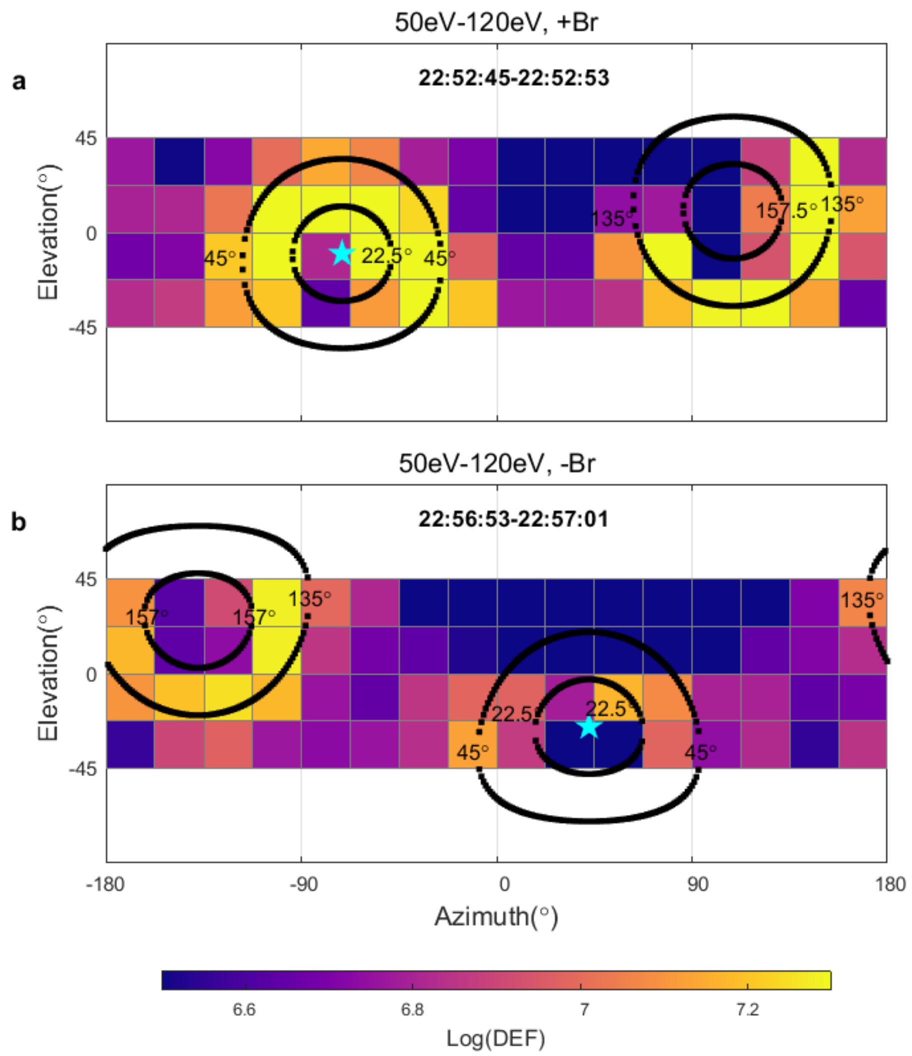

Supplementary Figure 3. SWIA observations of the angular distribution of the dispersed ions with energy ranging from 50-120 eV. a: the observed angular distribution with positive Br during 22:52:45-22:52:53 UTC. b: the observed angular distribution with negative Br during 22:52:45-22:52:53 UTC. The cyan pentagram represents the direction of the local magnetic field. The black circles represent the directions with a pitch angle of 22.5°, 45°, 135°, and 157.5°.

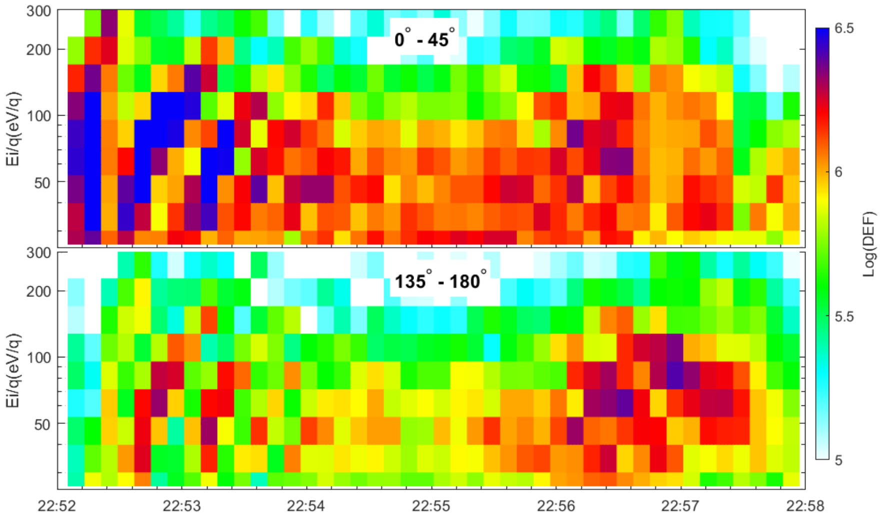

Supplementary Figure 4. SWIA observations of the differential energy flux of dispersed ions at 0-45° (upper panel) and 135°-180° (bottom panel) pitch angles. The dispersed structures occur simultaneously in both parallel and antiparallel moving directions, which contradicts the scenario of periodicity caused by repeated bounce motions.

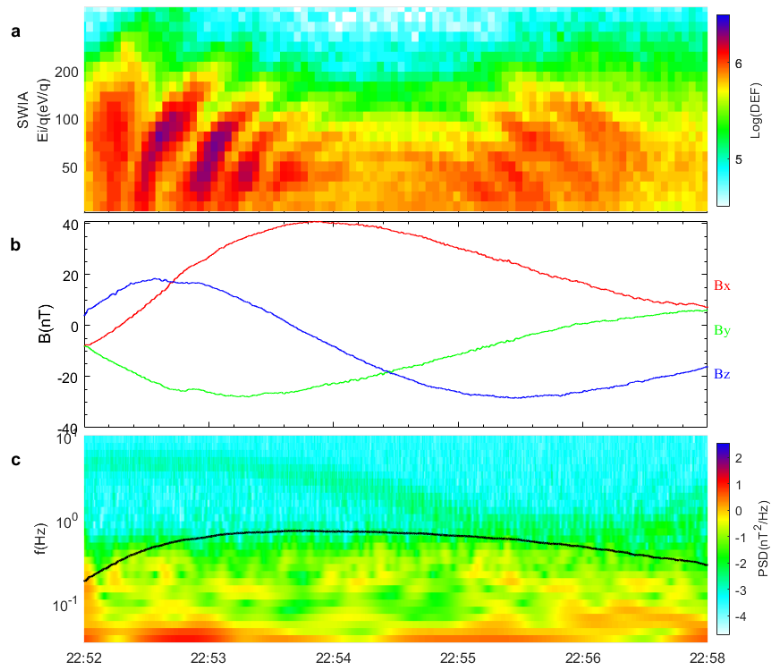

Supplementary Figure 5. Wave analysis. a: Ion spectrum. **b:** 32 Hz magnetic fields data. **c:** The power spectral density of the magnetic field. The black curve in c denotes the local gyro-frequency of protons. There are no obvious wave signatures during the observed event.

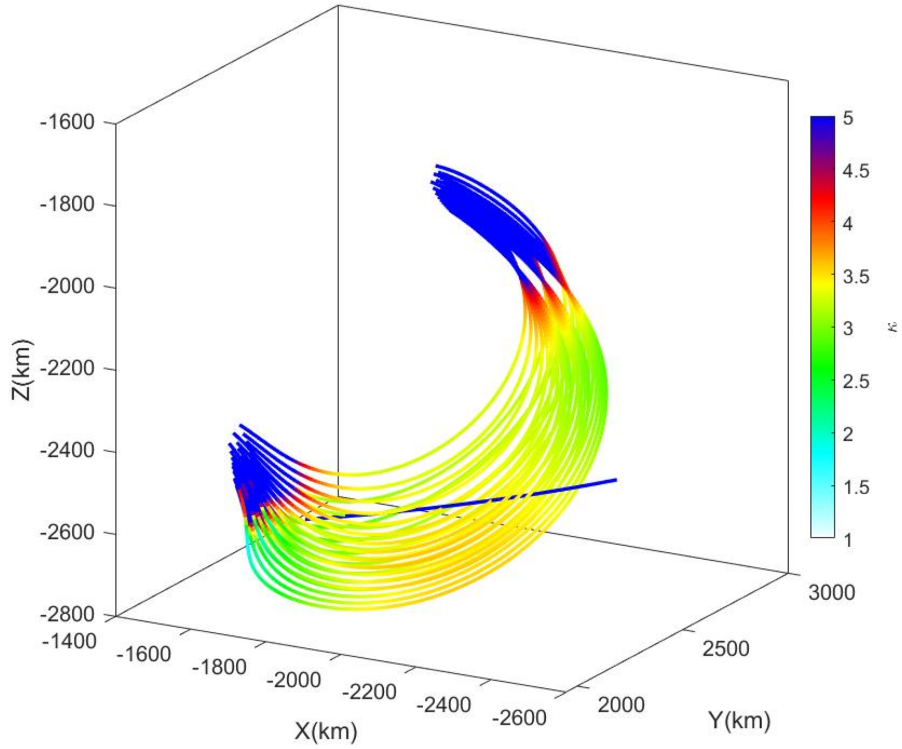

Supplementary Figure 6. The distribution of adiabatic parameter of 200 eV H$^+$ with pitch angle of 90° along the traced field lines. The blue lines are the MAVEN's trajectories. The adiabatic parameter, κ is defined as the square root of the ratio between the value of magnetic field curvature radius and the particle's Larmor radius (Büchner & Zelenyi, 1989), that is $\kappa = \sqrt{|\overrightarrow{R_c}|/r_g}$, where $\overrightarrow{R_c}$ is the local curvature radius of field lines, that is $\overrightarrow{R_c} = \left((\vec{b} \cdot \nabla)\vec{b}\right)^{-1}$. r_g denotes the gyroradius of particles, that is $r_g = mV_{\perp}/Bq$. The particles basically adhere to an adiabatic motion for $\kappa \gg 1$, because the gyroradius of particles is negligible compared with the spatially variable scale of magnetic fields.

Supplementary Table 1. The list of the wedge-like dispersion events.

No	Time	Rising tone (Yes?)	Falling tone (Yes?)	Solar wind dynamic pressure
1	2015-08-03 10:37:45-10:41:30	Y	Y	1.47
2	2015-12-05 08:24:00-08:31:00	Y	Y	-
3	2018-02-07 10:54:00-11:00:00	Y	Y	0.65
4	2018-02-25 17:38:30-17:41:00	Y		1.3
5	2018-04-15 22:52:00-22:58:00	Y	Y	3.03
6	2018-05-06 00:51:50-00:54:30	Y	Y	-
7	2018-05-31 21:14:20-21:17:30	Y	Y	-
8	2018-07-03 12:34:37-12:35:52	Y		0.30
9	2018-07-15 17:57:45-17:59:15	Y		0.47
10	2018-07-17 18:49:15-18:56:00	Y	Y	0.32
11	2019-03-21 19:57:45-19:59:15	Y		0.52
12	2019-03-23 21:22:00-21:24:00	Y		0.65
13	2019-05-16 03:34:30-03:40:00	Y	Y	0.23
14	2019-06-02 01:27:00-01:29:30	Y	Y	0.97
15	2019-09-03 17:49:30-17:51:15	Y		-
16	2020-04-29 21:27:00-21:29:00	Y	Y	0.71
17	2020-05-20 14:38:00-14:42:00	Y		-

References

Büchner, J., & Zelenyi, L. M. (1989). Regular and chaotic charged particle motion in magnetotail like field reversals: 1. Basic theory of trapped motion. Journal of Geophysical Research, 94(A9). https://doi.org/10.1029/JA094iA09p11821

Gao, J. W., Rong, Z. J., Lucy, K., Li, X. Z., Liu, D., & Wei, Y. (2021). A spherical harmonic Martian crustal magnetic field model combining data sets of MAVEN and MGS. Earth and Space Science, 8(10), e2021EA001860. https://doi.org/10.1029/2021EA001860

Trotignon, J. G., Mazelle, C., Bertucci, C., & Acuña, M. H. (2006). Martian shock and magnetic pile-up boundary positions and shapes determined from the Phobos 2 and Mars Global Surveyor data sets. Planetary and Space Science, 54(4), 357–369. https://doi.org/10.1016/j.pss.2006.01.003

Xu, S., Weber, T., Mitchell, D. L., Brain, D. A., Mazelle, C., DiBraccio, G. A., & Espley, J. (2019). A Technique to Infer Magnetic Topology at Mars and Its Application to the Terminator Region. Journal of Geophysical Research: Space Physics, 124(3), 1823-1842. https://doi.org/10.1029/2018ja026366